

Received December 29, 2019; reviewed; accepted February 15, 2019

Adsorption of lead ion on the hydrated rutile (110) surface: a DFT calculation study

Heng Zou¹, Qinbo Cao^{1,2}, Xiumin Chen^{1,2}, Dianwen Liu^{1,2}

¹ Faculty of Land Resources Engineering, Kunming University of Science and Technology, Kunming 650093, Yunnan, PR China

² State Key Laboratory of Complex Nonferrous Metal Resources Clean Utilization, Kunming 650093

Corresponding authors: cabdxx@163.com; (Qinbo Cao); ldwkust@126.com (Dianwen Liu)

Abstract: The adsorption behavior of lead species on the hydrated rutile surface was investigated with inductively coupled plasma mass spectrometry (ICP-MS) measurements and density functional theory (DFT) calculations. ICP-MS experiments suggested that lead species can be readily absorbed by the rutile powder in water at pH 6.5. From the ICP-MS results and the species distribution of Pb^{2+} , it was concluded that Pb^{2+} was the major lead species adsorbing at the rutile/water interface at the pH of 6.5. DFT calculation results indicated that Pb^{2+} could adsorb at four different sites on the surface. At each site, water molecules or OH groups were involved in the reaction with Pb^{2+} . The water molecules/OH groups on the rutile surface play an important role during the adsorption of Pb^{2+} on the hydrated rutile surface.

Keywords: rutile, hydrated surface, lead ion, adsorption, density functional theory

1. Introduction

Rutile ore is an important source for the production of titanium metal and titanium pigment (Bulatovic and Wyslouzil, 1999; Gázquez et al., 2014). Motivated by the growing commercial demand for titanium products, the beneficiation of rutile ore has received much attention in the past decade.

Commonly, rutile ore can be upgraded with gravity and magnetic separation methods and also flotation techniques (Chachula and Liu, 2003; Liu and Peng, 1999; Terzi and Kursun, 2015). While, flotation is much more efficient than other techniques to enrich rutile from its deposit.

Great efforts have been made to improve the flotation efficiency of rutile. Oleate is a satisfactory collector for rutile flotation. The rutile recovery reached 85.27% at pH 7.5 with oleate (Wang et al., 2014). While, rutile flotation plants prefer to use more selective collectors, such as benzyl arsenic acid and salicyl hydroxamic acid (SHA). It has been found that Pb^{2+} is an efficient activator for the flotation of rutile with SHA at neutral pH. The adsorption of SHA on the rutile surface can be significantly enhanced by the addition of $Pb(NO_3)_2$ into the slurry at pH 6.3 (Li et al., 2016).

Recently, the activation behaviors of Pb^{2+} for some oxide minerals has attracted considerable interest (Tian et al., 2018). It was found that Pb^{2+} can be used as an activator in the flotation of quartz, scheelite and cassiterite (Feng et al., 2017; Liu et al., 2016; Ren et al., 2017; Zhao et al., 2015). With regard to titanium-bearing minerals, Pb^{2+} can dramatically improve the flotation of ilmenite (Chen et al., 2017; Fan and Rowson, 2000; Xu et al., 2017). In the case of rutile, Li et al. has investigated the adsorption behavior of Pb^{2+} on the rutile surface using experimental methods (Li et al., 2016).

The rutile surface shows a strong affinity toward water molecules. Thus, the rutile surface is highly hydrophilic in water (Watanabe et al., 1999). The bound water molecules on the rutile surface play an important role in many industrial applications of rutile (Konstantinou and Albanis, 2004). However, the adsorption features of water molecules on the rutile surface are complex. Considerable studies have been devoted to revealing the adsorption structure of water on the rutile surface (Diebold, 2003; Předota et al., 2004; Zhang et al., 2008). It has been established that water molecules can directly adsorb on the rutile surface (Perron et al., 2007c). Meanwhile, some water molecules are dissociated on

the surface to generate hydroxyl (OH) groups. These results are also supported by an ab initio molecular dynamics study (Agosta et al., 2017). It is reasonable to expect that water molecules/OH groups on the rutile surface may affect the adsorption of Pb^{2+} onto the mineral surface. However, such effect is difficult to be fully revealed by ex-situ experimental methods.

By contrast to experimental techniques, density functional theory (DFT) calculations can provide a detailed picture about the adsorption of a metal ion on the hydrated rutile surface. Previous DFT studies focused on the adsorption mechanism of calcium ion on the rutile surface, because this issue is important to understand the bioactivity of titanium implants (Lu et al., 2007). It was found that calcium ion binds with two OH groups on a partially hydroxylated rutile (110) surface (Svetina et al., 2001). Further study indicated that the adsorption of calcium atom on the hydrated rutile surface is more stable than that on the dry rutile surface (Lu et al., 2010). These findings clearly indicated that the water molecules and OH groups on the rutile surface are involved in the interaction between a metal ion and the rutile surface. Whereas, few researchers have addressed the binding features of Pb^{2+} on the hydrated rutile surface.

The binding behavior of Pb^{2+} on the rutile surface at neutral pH is crucial to understand the activation mechanism of Pb^{2+} for the rutile flotation with SHA. The aim of this study is to examine the interaction between Pb^{2+} and the rutile surface in the flotation system. Firstly, the major Pb species on the rutile surface was assessed by the inductively coupled plasma mass spectrometry tests. Further, the binding structures of Pb^{2+} on the hydrated rutile were investigated with DFT calculations.

2. Materials and methods

2.1. Sample and reagents

Pure rutile pebbles (93% of purity) were obtained from Kunming Metallurgical Research Institute, China. The X-ray diffraction (XRD) pattern shows that only the diffraction peaks of rutile were detected for the sample (Fig. 1). Lead nitrate, hydrochloric acid and sodium hydrate were all AR grade and were purchased from Sinopharm Chemical Reagent Co., Ltd., China. Dilute HCl and NaOH solutions (0.1 mol/dm^3) were used to adjust the pH of the rutile slurry.

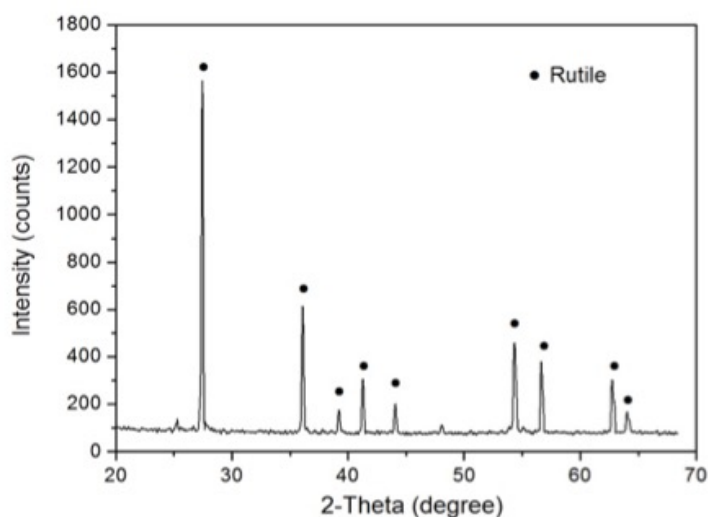


Fig. 1 XRD pattern of the rutile sample

2.2. ICP-MS tests

A NexION 350X (PerkinElmer, Inc.) was used in the inductively coupled plasma mass spectrometry (ICP-MS) experiments. Rutile powder (38–75 μm , 2 g) was added into 100 cm^3 of deionized water. The suspension was stirred for 3 min. Further, desired amount of $\text{Pb}(\text{NO}_3)_2$ was added into the slurry. The conditioning time for the $\text{Pb}(\text{NO}_3)_2$ was 3 min. After the conditioning, the rutile slurry was centrifuged to obtain a clear solution for the ICP-MS test. Each sample was measured three times, and the error was less than 10%. The pH of the rutile suspension was controlled at 6.5.

2. 3. Theoretical calculations

All calculations were carried out with the Cambridge Sequential Total Energy Package (CASTEP) code, which is based on the density functional theory (DFT) (Segall et al., 2002). Generalized gradient approximation (GGA) using the scheme of the Perdew-Burke-Ernzerhof functional was used to treat the exchange and correlation potentials (Perdew et al., 1996; Perdew and Zunger, 1981). The interactions between the ionic core and valence electrons were described with ultrasoft pseudopotentials (Francis and Payne, 1990). The valence electron configurations for the elements considered in the study were H 1s¹, O 2s² 2p⁴, Ti 3s² 3p⁶ 3d² 4s² and Pb 5d¹⁰ 6s² 6p². Spin-polarization calculations were performed during the simulation. The energy convergence was set as 1×10⁻⁶ eV/atom. The Brillouin-zone integrations were performed using a 2×2×1 k-point grid. A kinetic energy cutoff of 400 eV was used for the calculations. Using convergence tests, the k-point grid and cutoff energy were found to be sufficient to obtain numerical convergence.

All of the structures were optimized using the Broyden-Fletcher-Goldfarb-Shanno (BFGS) method, and the convergence criteria for the geometric optimization were set to (a) an energy tolerance of 1×10⁻⁵ eV/atom; (b) a maximum force tolerance of 0.03 eV/Å; (c) a maximum displacement tolerance of 0.001 Å. All of the atoms were allowed to relax during the calculation.

The adsorption energy (ΔE_{ads}) of Pb²⁺ at the rutile surface was calculated according to the following equation:

$$\Delta E_{\text{ads}} = E_{\text{adsorbate+slab}} - E_{\text{adsorbate}} - E_{\text{slab}} \quad (2)$$

where $E_{\text{adsorbate+slab}}$ and E_{slab} are the total energies of the rutile surface model after and before the adsorption of Pb²⁺, respectively, and $E_{\text{adsorbate}}$ is the energy of Pb²⁺. The energy of Pb²⁺ was calculated at the gamma-point by placing a Pb²⁺ ion in a cubic cell that has the same cell parameters as that of the surface model. The (110) plane was used to simulate the interaction between Pb²⁺ and the surface, since the (110) plane is the most stable plane (Perron et al., 2007a).

3. Results and discussion

3. 1. ICP-MS analysis

Table 1 reports the lead concentration in the rutile slurry after the conditioning with Pb(NO₃)₂. At each examined Pb(NO₃)₂ dosage, more than 85% of Pb species was absorbed by the rutile particles. It appeared that Pb species could readily adsorb onto the rutile surface at the pH of 6.5, which is consistent with a previous report (Li et al., 2016). However, ICP-MS can only measure the total concentration of the Pb species. The concentration of a particular Pb species in the solution cannot be determined by this method. According to the distribution diagram of Pb²⁺ in the solution (Weng, 2004), Pb²⁺ and Pb(OH)⁺ both occurred in the solution at pH 6.5 (Fig. 2). However, their distribution coefficients are different. At the pH of 6.5, Pb²⁺ was the dominant species in the solution, and was 84 mol% in total. By contrast, only 16 mol% of the Pb species were in the form of Pb(OH)⁺. It is reasonable to expect that Pb²⁺ is the dominant species adsorbing on the rutile surface.

Table 1 Pb concentrations (mol/dm³) in the rutile slurry after the conditioning with Pb(NO₃)₂.

Pb(NO ₃) ₂ dosage	Residual concentration of Pb	Concentration reduction
7.5×10 ⁻⁶	1.1×10 ⁻⁶	85.2%
2.5×10 ⁻⁵	1.6×10 ⁻⁶	93.6%
5.0×10 ⁻⁵	4.8×10 ⁻⁶	90.4%
1.0×10 ⁻⁴	7.0×10 ⁻⁷	99.3%
2.0×10 ⁻⁴	7.0×10 ⁻⁶	96.5%

To further understand the adsorption mechanism of Pb²⁺ on the rutile surface, DFT calculations were performed to evaluate the interaction between Pb²⁺ and the rutile surface in the following section.

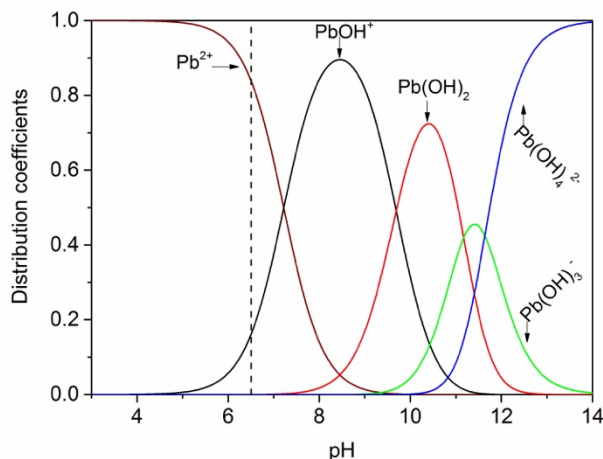


Fig. 2 Distribution of lead hydroxyl species in water as a function of pH

3. 2. Hydrated rutile (110) surface

The first hydration layer on the rutile (110) surface at neutral pH has been well-established with the DFT calculation (Perron et al., 2007b). Water molecules can adsorb on top sites of the five-fold-coordinated (5f) Ti atoms on the rutile surface; Further, 10-25 mol% of water molecules on the surface may dissociate into OH groups and H atoms (Brinkley et al., 1998; Perron et al., 2007b). Consequently, the OH group from a dissociated water molecule can bind to the Ti(5f) atom, while the H atom from the dissociated water molecule can interact with a nearby bridging (br) O atom to generate an OH group.

Based on these findings, the rutile (110) surface with first hydration layer was generated as shown in Fig. 3. This surface is a reasonable representation of the rutile surface with the first hydration layer (Perron et al., 2007b). It was observed that H-bonds occurred between the water molecules on this hydrated rutile surface (Fig. 3). In addition, water molecule also donated an H-bond to a nearby O(br) atom. As a result, a chain-like structure of H-bond was produced on the rutile surface. It is expected that such H-bond structure and also water molecules on the rutile surface are not benefit for the adsorption of SHA on the rutile surface. Therefore, Pb^{2+} is necessary to be used as an activator for the rutile flotation.

Pb^{2+} was further placed on the hydrated rutile surface at various initial sites to examine the possible interaction models. To better describe the binding structures, interactional oxygen atoms on the rutile surface were numbered as shown in Fig. 4.

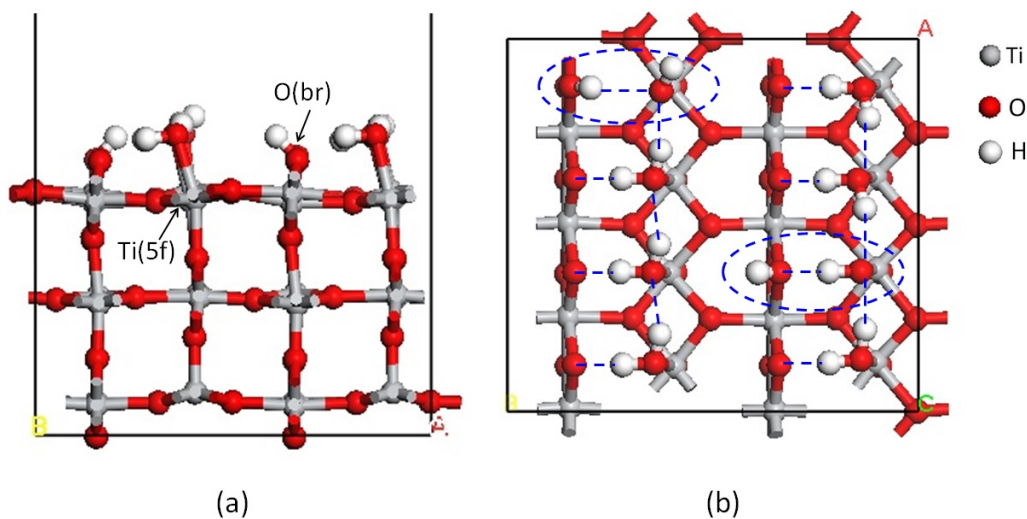


Fig. 3 Optimized structure of the hydrated rutile (110) surface: (a) side view; (b) top view. H-bonds and OH groups generated by the dissociation of water molecules are marked by blue dash lines

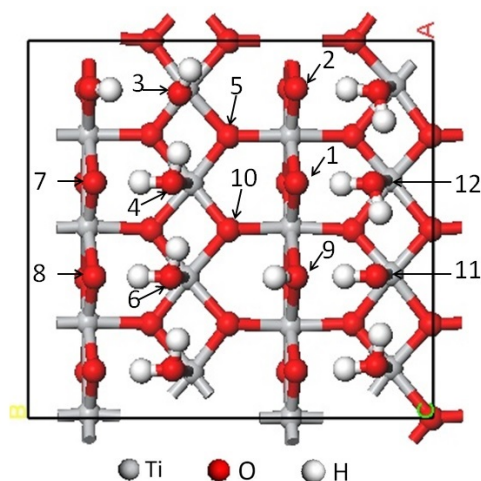


Fig. 4 Numbered O atoms on the hydrated rutile (110) surfaces

3. 3. Binding structure of Pb^{2+} on the hydrated rutile surface

Four different sites on the hydrated rutile (110) surface allowed for the adsorption of Pb^{2+} ion, including three four-fold hollow (4FH1-4FH3) sites and one three-fold hollow (3FH) site, as shown in Fig. 5.

At the 4FH1 site, Pb^{2+} was bound to three O atoms (O1, O2 and O5) and one OH group on the rutile surface (Fig. 6a). At the 4FH2 site, Pb^{2+} interacted with four OH groups, namely, the $\text{O}_{(4)}\text{H}$, $\text{O}_{(6)}\text{H}$, $\text{O}_{(7)}\text{H}$ and $\text{O}_{(8)}\text{H}$ groups (Fig. 6b). It should be stressed that two water molecules, i.e., $\text{H}_2\text{O}_{(4)}$ and $\text{H}_2\text{O}_{(6)}$, were present on the rutile surface before the interaction with Pb^{2+} . These water molecules were dissociated due to the adsorption of Pb^{2+} at the 4FH2 site; consequently, four new OH groups were generated on the rutile surface. At the 4FH3 site, Pb^{2+} coordinated with O1 and two OH groups (Fig. 7a). In addition, Pb^{2+} could also locate at the 3FH site interacting with O1, O10 and $\text{O}_{(9)}\text{H}$ group (Fig. 7b). Such results evidently suggest that water molecules/OH groups on the rutile surface were involved in the reaction between the rutile surface and Pb^{2+} .

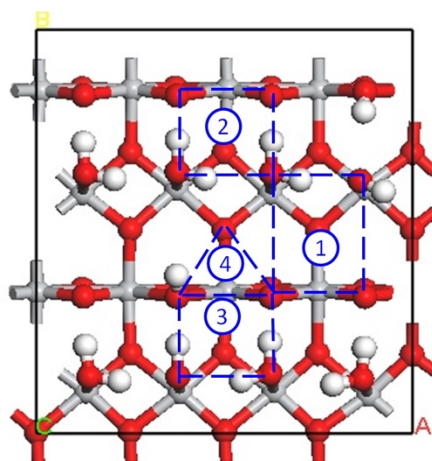


Fig. 5 Three four-fold hollow (4FH) sites and one three-fold hollow (3FH) site on the hydrated rutile (110) surface: (1) 4FH1 site; (2) 4FH2 site; (3) 4FH3 site; (4) 3FH site.

The adsorption of Pb^{2+} on the hydrated rutile (110) surface generated Pb–O bonds. The Pb–O bond lengths were in the range from 2.23 Å to 2.55 Å (Table 2). On the other hand, the adsorption energies were all negative, as shown in Table 2. It indicates that the adsorption of Pb^{2+} on the hydrated rutile surface is energetically favorable, which is in line with the above ICP-MS results. Further, the 4FH1 site was the most stable site for the adsorption of Pb^{2+} , due to the lowest adsorption energy at this site.

Our DFT calculations imply that the hydration state on the rutile surface can significantly affect the

adsorption behavior of Pb^{2+} . In fact, the water molecules and/or OH groups on the rutile surface can react with Pb^{2+} during its adsorption onto the hydrated rutile surface. In addition, the effects of bulk water and the hydration of Pb^{2+} on the interaction between the rutile surface and the Pb^{2+} were not considered in this work. Such effects should be investigated in future.

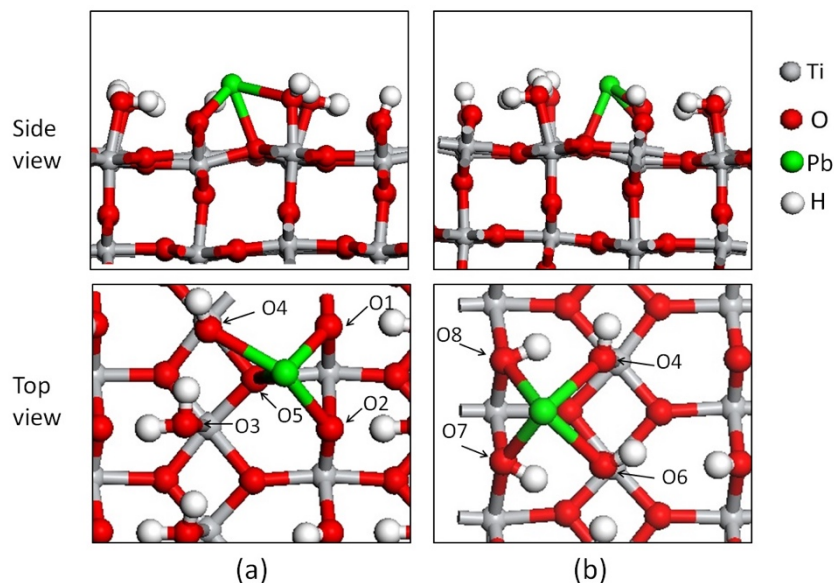


Fig. 6 Binding structures of Pb^{2+} on the hydrated rutile (110) surface: (a) at the four-fold hollow (4FH1) site of O1, O2, O₍₄₎H and H₂O₍₃₎; (b) at the four-fold hollow (4FH2) site of O₍₄₎H, O₍₆₎H, O₍₇₎H and O₍₈₎H groups

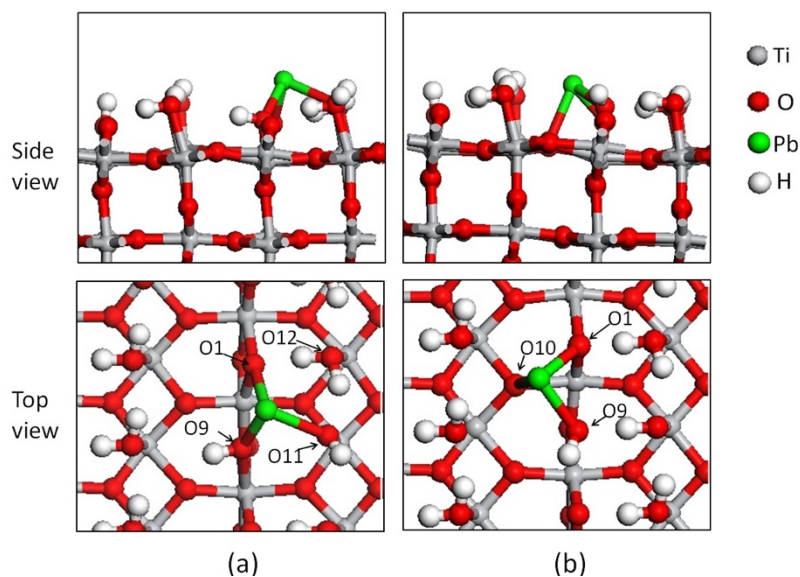


Fig. 7 Binding structures of Pb^{2+} on the hydrated rutile (110) surface: (a) at the four-fold hollow (4FH3) site of O1, O₍₉₎H, O₍₁₁₎H and H₂O₍₁₂₎; (b) at the three-fold hollow (3FH) site of O1, O10 and O₍₉₎H

Table 2 Adsorption energies and bond lengths for Pb^{2+} adsorbing at the hydrated rutile (110) surface

Site	ΔE_{ads} (kJ/mol)	Bond lengths (Å)			
4FH1	-2112.32	Pb-O1(2.28)	Pb-O2(2.42)	Pb-O4(2.55)	Pb-O5(2.49)
4FH2	-2072.96	Pb-O4(2.46)	Pb-O6(2.48)	Pb-O7(2.46)	Pb-O8(2.43)
4FH3	-2066.40	Pb-O1(2.28)	Pb-O9(2.26)	Pb-O11(2.42)	
3FH	-2065.91	Pb-O1(2.23)	Pb-O9(2.35)	Pb-O10(2.42)	

3. 4. PDOS analysis

The adsorption of Pb^{2+} on the hydrated surface generated Pb–O bonds. The covalent character of Pb–O bonds can be interpreted using the partial density of states (PDOS) analysis, because this analysis reveals the interactions between the orbitals of bonding atoms. We only reported the PDOS results of the most stable structure, i.e., the adsorption structure at the 4FH1 site.

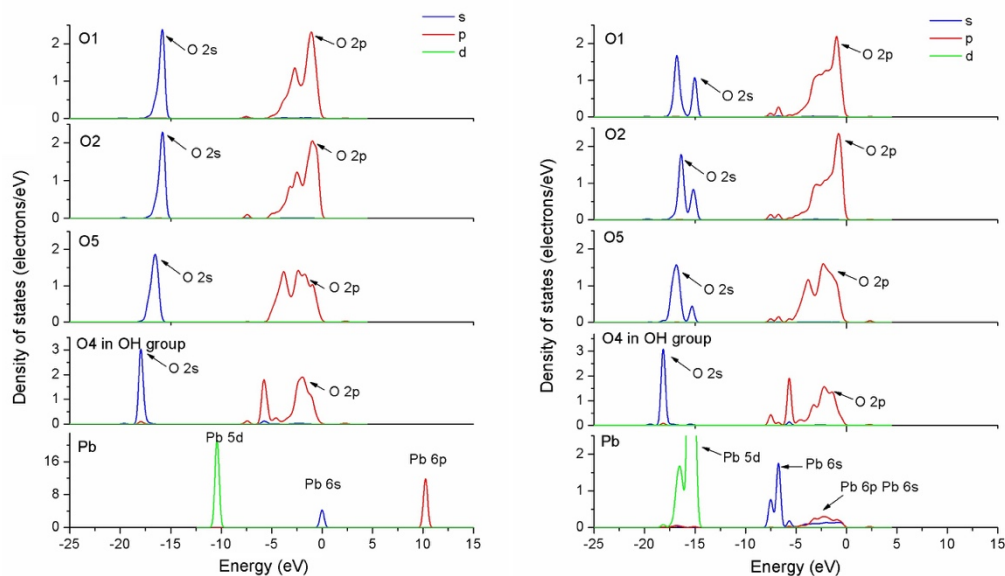


Fig. 8 PDOS diagrams of O1, O2, O5, O4 and Pb^{2+} before (left) and after (right) the interaction

At the 4FH1 site, Pb^{2+} was coordinated to four oxygen atoms including three O_{bulk} atoms (O1, O2 and O5) and the O4 atom in $\text{O}_{(4)}\text{H}$ group. For a interactional O_{bulk} atom, due to the interaction with Pb^{2+} , the PDOS peak of O 2p orbital changed to overlap with the Pb 6s and Pb 6p orbitals (Fig. 8). This result indicates that a strong hybridization occurred between these orbitals.

On the other hand, for each interacting O_{bulk} atom, the peak of O 2s orbital was at -17 eV before the interaction with Pb^{2+} ; after the interaction, the peak of O 2s orbital split into two peaks within the energy range from -17 eV to 15 eV. As a result, the O 2s orbital overlapped well with the Pb 5d orbital, indicating a strong hybridization between them. In contrast, the interaction between Pb^{2+} and $\text{O}_{(4)}\text{H}$ barely changed the 2s state of $\text{O}_{(4)}$. In fact, the 2s peak of $\text{O}_{(4)}$ located at a deeper level in the conduction band comparing with that of each interactional O_{bulk} . For this reason, the 2s orbital of $\text{O}_{(4)}$ was less reactive.

The PDOS results show that the covalent character is strong in the Pb–O bond formed on the hydrated rutile surface. For this reason, Pb^{2+} can adsorb onto the hydrated rutile surface stably. In addition, it is expected Pb^{2+} may act like a bridge for the further adsorption of SHA. Future DFT calculation work will focus on the adsorption of SHA on the Pb-activated rutile surface.

4. Conclusions

Pb^{2+} could readily adsorb onto the rutile surface at pH 6.5. On the hydrated rutile surface, there were four sites allowing for the adsorption of Pb^{2+} . At each site, Pb^{2+} interacted with the O atoms in the rutile lattice and the OH groups on the hydrated surface; hence, Pb–O bonds were generated on the hydrated rutile (110) surface. The formation of these Pb–O bonds was depended on the hybridization of O 2s and Pb 5d orbitals and also the interaction between O 2p, Pb 6s and Pb 6p orbitals. It is expected that Pb atom on the hydrated rutile surface may act as a bridge for the further adsorption of a collector.

Acknowledgments

The financial support from the Analysis and Testing Foundation of Kunming University of Science and Technology is gratefully acknowledged.

References

- AGOSTA, L., BRANDT, E.G., LYUBARTSEV, A.P., 2017. *Diffusion and reaction pathways of water near fully hydrated TiO₂ surfaces from ab initio molecular dynamics*. Journal of Chemical Physics 147, 37.
- BRINKLEY, D., DIETRICH, M., ENGEL, T., FARRALL, P., GANTNER, G., SCHAPE, A., SZUCHMACHER, A., 1998. *A modulated molecular beam study of the extent of H₂O dissociation on TiO₂ (110)*. Surface Science 395, 292-306.
- BULATOVIC, S., WYSLOUZIL, D.M., 1999. *Process development for treatment of complex perovskite, ilmenite and rutile ores*. Minerals Engineering 12, 1407-1417.
- CHACHULA, F., LIU, Q., 2003. *Upgrading a rutile concentrate produced from Athabasca oil sands tailings*. Fuel 82, 929-942.
- CHEN, P., ZHAI, J., SUN, W., HU, Y., YIN, Z., 2017. *The activation mechanism of lead ions in the flotation of ilmenite using sodium oleate as a collector*. Minerals Engineering 111, 100-107.
- DIEBOLD, U., 2003. *The surface science of titanium dioxide*. Surface Science Reports 48, 53-229.
- FAN, X., ROWSON, N. A., 2000. *The effect of Pb(NO₃)₂ on ilmenite flotation*. Minerals Engineering 13, 205-215.
- FENG, Q., ZHAO, W., WEN, S., CAO, Q., 2017. *Activation mechanism of lead ions in cassiterite flotation with salicylhydroxamic acid as collector*. Separation and Purification Technology 178, 193-199.
- FRANCIS, G., PAYNE, M., 1990. *Finite basis set corrections to total energy pseudopotential calculations*. Journal of Physics: Condensed Matter 2, 4395.
- GAZQUEZ, M.J., BOLIVAR, J.P., CARCIATENORIO, R., VACA, F., 2014. *A Review of the Production Cycle of Titanium Dioxide Pigment*. Materials Sciences & Applications 05, 441-458.
- KONSTANTINOU, I.K., ALBANIS, T.A., 2004. *TiO-assisted photocatalytic degradation of azo dyes in aqueous solution: kinetic and mechanistic investigations: A review*. Applied Catalysis B Environmental 49, 1-14.
- LI, H., MU, S., WENG, X., ZHAO, Y., SONG, S., 2016. *Rutile flotation with Pb²⁺ ions as activator: Adsorption of Pb²⁺ at rutile/water interface*. Colloids and Surfaces A: Physicochemical and Engineering Aspects 506, 431-437.
- LIU, B., WANG, X., DU, H., LIU, J., ZHENG, S., ZHANG, Y., MILLER, J.D., 2016. *The surface features of lead activation in amyl xanthate flotation of quartz*. International Journal of Mineral Processing 151, 33-39.
- LIU, Q., PENG, Y., 1999. *The development of a composite collector for the flotation of rutile*. Minerals Engineering 12, 1419-1430.
- LU, X., ZHANG, H.P., LENG, Y., FANG, L., QU, S., FENG, B., WENG, J., HUANG, N., 2010. *The effects of hydroxyl groups on Ca adsorption on rutile surfaces: a first-principles study*. J Mater Sci Mater Med 21, 1-10.
- LU, X., ZHAO, Z., LENG, Y., 2007. *Biomimetic calcium phosphate coatings on nitric-acid-treated titanium surfaces*. Materials Science & Engineering C 27, 700-708.
- PERDEW, J.P., BURKE, K., ERNZERHOF, M., 1996. *Generalized gradient approximation made simple*. Physical review letters 77, 3865.
- PERDEW, J.P., ZUNGER, A., 1981. *Self-interaction correction to density-functional approximations for many-electron systems*. Physical Review B 23, 5048.
- PERRON, H., DOMAIN, C., ROQUES, J., DROT, R., SIMONI, E., CATELETTE, H., 2007a. *Optimisation of accurate rutile TiO₂ (110), (100), (101) and (001) surface models from periodic DFT calculations*. Theoretical Chemistry Accounts Theory Computation & Modeling 117, 565-574.
- PERRON, H., VANDENBORRE, J., BOMAIN, DROT, R., ROQUES, J., SIMONI, E., EHRHARDT, J.J., CATELETTE, H., 2007b. *Combined investigation of water sorption on TiO₂ rutile (1 1 0) single crystal face: XPS vs. periodic DFT*. Surface Science 601, 518-527.
- PREDOTA, M., BANDURA, A.V., CUMMINGS, P.T., KUBICKI, J.D., WESOLOWSKI, D.J., CHIALVO, A.A., MACHESKY, M.L., 2004. *Electric Double Layer at the Rutile (110) Surface. 1. Structure of Surfaces and Interfacial Water from Molecular Dynamics by Use of ab Initio Potentials*. The Journal of Physical Chemistry B 108, 12049-12060.
- REN, LL, QIU, H., ZHANG, M., FENG, K., LIU, P., GUO, J., FENG, J., 2017. *Behavior of Lead Ions in Cassiterite Flotation Using Octanohydroxamic Acid*. Industrial & Engineering Chemistry Research 56,

8723-8728.

- SEGALL, M., LINDAN, P.J., PROBERT, M.A., PICHARD, C., HASNI, P., CLARK, S, PAYNE, M., 2002. *First-principles simulation: ideas, illustrations and the CASTEP code*. Journal of Physics: Condensed Matter 14, 2717.
- SVETINA, M., CIACCHI, L.C., SBAIZERO, O., MERIANI, S., VITA, A.D., 2001. *Deposition of calcium ions on rutile (110): a first-principles investigation*. Acta Materialia 49, 2169-2177.
- TERZI, M., KURSUN, I., 2015. *Investigation of recovery possibilities of rutile minerals from the feldspar tailings with gravity separation methods*. Russian Journal of Non-Ferrous Metals 56, 235-245.
- TIAN, M., GAO, Z., SUN, W., HAN, H, SUN, L., HU, Y., 2018. *Activation role of lead ions in benzohydroxamic acid flotation of oxide minerals: New perspective and new practice*. Journal of Colloid & Interface Science.
- WANG, J., CHENG, H.W., ZHAO, H.B., QIN, W.Q., QIU, G.Z., 2014. *Flotation behavior and mechanism of rutile in presence of sodium oleate*. Chinese Journal of Nonferrous Metals 24, 820-825.
- WATANABE, T., NAKAJINA, A., WANG, R., MINABE, M., KOIZUMI, S., FUJISHIMA, A., HASHIMOTO, K., 1999. *Photocatalytic activity and photoinduced hydrophilicity of titanium dioxide coated glass*. Thin Solid Films 351, 260-263.
- WENG, C.H., 2004. *Modeling Pb(II) adsorption onto sandy loam soil*. Journal of Colloid & Interface Science 272, 262-270.
- XU, L., TIAN, J., WU, H., LU, Z., YANG, Y., SUN, W., HU, Y., 2017. *Effect of Pb²⁺ ions on ilmenite flotation and adsorption of benzohydroxamic acid as a collector*. Applied Surface Science 425.
- ZHANG, W., YANG, J., LUO, Y., MONTI, S., CARRAVETTA, VL, 2008. *Quantum molecular dynamics study of water on TiO₂(110) surface*. Journal of Chemical Physics 129, 064703.
- ZHAO, G., WANG, S., ZHONG, H., 2015. *Study on the activation of scheelite and wolframite by lead nitrate*. Minerals 5, 247-258.